

Article

Causality Analysis for COVID-19 among Countries Using Effective Transfer Entropy

Baki Ünal 

Industrial Engineering Department, Faculty of Engineering and Natural Sciences, İskenderun Technical University, İskenderun 31200, Hatay, Turkey; bakiunal@gmail.com

Abstract: In this study, causalities of COVID-19 across a group of seventy countries are analyzed with effective transfer entropy. To reveal the causalities, a weighted directed network is constructed. In this network, the weights of the links reveal the strength of the causality which is obtained by calculating effective transfer entropies. Transfer entropy has some advantages over other causality evaluation methods. Firstly, transfer entropy can quantify the strength of the causality and secondly it can detect nonlinear causal relationships. After the construction of the causality network, it is analyzed with well-known network analysis methods such as eigenvector centrality, PageRank, and community detection. Eigenvector centrality and PageRank metrics reveal the importance and the centrality of each node country in the network. In community detection, node countries in the network are divided into groups such that countries in each group are much more densely connected.

Keywords: COVID-19; causality analysis; causality network; transfer entropy; network analysis



Citation: Ünal, B. Causality Analysis for COVID-19 among Countries Using Effective Transfer Entropy. *Entropy* **2022**, *24*, 1115. <https://doi.org/10.3390/e24081115>

Academic Editors: Fan Yang and Wenkai Hu

Received: 4 July 2022

Accepted: 10 August 2022

Published: 13 August 2022

Publisher's Note: MDPI stays neutral with regard to jurisdictional claims in published maps and institutional affiliations.



Copyright: © 2022 by the author. Licensee MDPI, Basel, Switzerland. This article is an open access article distributed under the terms and conditions of the Creative Commons Attribution (CC BY) license (<https://creativecommons.org/licenses/by/4.0/>).

1. Introduction

Investigating causality and information flow between systems is an important area of research in the literature. To evaluate causality and information flow between systems, time series data generated by these systems are utilized. The most widely used causality analysis method in the literature was proposed by Granger [1] and is known as Granger causality. Following Granger, many causality tests are proposed in the literature by authors such as Toda–Yamamoto [2] and Hatemi-J [3] in their own causality tests. Furthermore, in the literature, many nonlinear causality analysis methods are presented [4–7]; however, all these methods are based on a hypothesis-testing procedure. In these procedures, a test statistic is computed and, according to the value of this statistic, the existence of causality is determined. Therefore, these methods do not measure the strength of causality with a numerical value. A new information-theory-based causality measure, transfer entropy, can measure the strength of the causality [8,9] and can also detect nonlinear causality relationships. In this study, a causality network is constructed using COVID-19 data from seventy countries and effective transfer entropy. The obtained network is a weighted directed network where the directions of links reflect the directions of causality relationships, and the weights of the links indicate the strength of the causalities measured with effective transfer entropy. In the transfer entropy methodology, two kinds of entropy type have been utilized in the literature. These are Shannon entropy and Rényi entropy. Rényi entropy has a free parameter which is denoted by q . When $q \rightarrow 1$, Rényi entropy converges to Shannon entropy. In this study, we utilized Shannon entropy in our transfer entropy calculations because Shannon entropy is more basic and does not require the selection of a free parameter which complicates the results. In the literature, there are many applications of Rényi entropy-based transfer entropy methodology [10–14]. Ultimately, we chose the transfer entropy methodology for the following reasons: First, unlike other causality assessment methods, transfer entropy not only detects whether there is causality but also measures the strength of this causality. Second, transfer entropy can detect nonlinear relations. Third, in

the literature, this methodology is successfully applied to many time series from different fields and its usefulness is proven. Fourth, there is a reliable software for computing transfer entropy.

After the construction of the causality network, this network is analyzed with network analysis methods such as eigenvector centrality, PageRank, and community detection. Eigenvector centrality and PageRank measure importance and centrality of nodes by assigning a numerical value to each node. In community detection, nodes in the network are divided into groups such that, in each group, the nodes are much more densely connected.

2. Materials and Methods

2.1. Transfer Entropy

Transfer entropy is an information-theory-based method to quantify information flow and causality between two systems. The concept of transfer entropy was independently formalized by both Thomas Schreiber [8] and Paluš et al. [9]. In the literature, in order to measure the interdependence between two systems, mutual information is purposed by Shannon and Weaver [15]. However, mutual information does not reveal dynamical and directional information. Transfer entropy possess properties of mutual information but also reflects dynamics of information flow (causality). Transfer entropy is based on Shannon entropy. Shannon entropy measures the average number of bits required to encode a discrete random variable, I , possessing the probability distribution $p(i)$ and is expressed with the following formula:

$$H_I = - \sum_i p(i) \log_2 p(i) \quad (1)$$

To obtain optimal encoding based on entropy, the probability distribution $p(i)$ must be known. The amount of bits which will be coded if a different distribution is utilized, such as when $q(i)$ is measured using Kullback entropy, is defined with the following formula [16]:

$$K_I = - \sum_i p(i) \log_2 p(i) / q(i) \quad (2)$$

Additionally, Kullback entropy for conditional probabilities is expressed with the following formula:

$$K_{IJ} = \sum_{i,j} p(i,j) \log \frac{p(i|j)}{q(i|j)} \quad (3)$$

If the two systems, assumed to be independent, corresponded, then Kullback entropy becomes:

$$M_{IJ} = \sum p(i,j) \log \frac{p(i,j)}{p(i)p(j)} \quad (4)$$

If transition probabilities are used instead of static probabilities, a dynamic structure can be revealed. For this, it is assumed that the system can be expressed by a Markov process of order k . This means that state i_{n+1} is independent of state i_{n-k} . In other words, $p(i_{n+1}|i_n, \dots, i_{n-k+1}) = p(i_{n+1}|i_n, \dots, i_{n-k+1}, i_{n-k})$. We note that $i_n^{(k)} = (i_n, \dots, i_{n-k+1})$. As a result, if the previous states are given an average number of bits required to encode an additional state, it is called the entropy rate and computed with the following formula:

$$h_I = - \sum p(i_{n+1}, i_n^{(k)}) \log(i_{n+1}, i_n^{(k)}) \quad (5)$$

In the expression above, $p(i_{n+1}, i_n^{(k)}) = p(i_{n+1}^{(k+1)}) / p(i_n^{(k)})$. To analyze information flow between systems, the entropy rate given above is generalized to more than one system by using following expression:

$$p(i_{n+1}, i_n^{(k)}) = p(i_{n+1}^{(k)}, j_n^{(l)}) \quad (6)$$

According to the expression above, if there is no information flow from J to I , the state of J will not affect the transition probabilities of I . If the expressions above are combined, then transfer entropy can be defined with the following formula:

$$T_{J \rightarrow I} = \sum p(i_{n+1}, i_n^{(k)}, j_n^{(l)}) \log \frac{p(i_{n+1} | i_n^{(k)}, j_n^{(l)})}{p(i_{n+1} | i_n^{(k)})} \tag{7}$$

The transfer entropy calculation described above has a deficiency for small samples. For small samples, the calculated transfer entropies are biased. To solve this problem, the concept of effective transfer entropy is suggested by Marschinski and Kantz [17]. To calculate an effective transfer entropy time, a series of observations from system J are shuffled. From this shuffled data, a transfer entropy is calculated. Then, the transfer entropy obtained from the shuffled data is subtracted from the transfer obtained from the original data. This method can be expressed as follows:

$$ET_{J \rightarrow I}(k, l) = T_{J \rightarrow I}(k, l) - T_{J_{Shuffled} \rightarrow I}(k, l) \tag{8}$$

In the expression above, $ET_{J \rightarrow I}(k, l)$ denotes effective transfer entropy and $T_{J_{Shuffled} \rightarrow I}(k, l)$ denotes transfer entropy calculated from shuffled data. With this shuffling procedure, the dependencies in J and between I and J are eliminated. If the sample size is increased, $T_{J_{Shuffled} \rightarrow I}(k, l)$ approaches zero. Therefore, $T_{J_{Shuffled} \rightarrow I}(k, l)$ displays the impact of a small sample size.

The statistical significances of calculated transfer entropies can be evaluated by using a block bootstrap method suggested by Dimpfl and Peter [18]. This method generates the p-values and transfer entropy distribution for the null hypothesis where there is no information flow.

To be used in the calculation of transfer entropy, data should be discrete. Data should be discretized if it is not discrete. To convert a continuous dataset to a discrete dataset, a procedure called symbolic recoding can be used. In this procedure, continuous data are partitioned into bins and each value in the continuous data is assigned to a bin. To perform this procedure, the bounds of the bins should be determined. If these boundaries are determined as q_1, q_2, \dots, q_n ($q_1 < q_2 < \dots < q_n$), a continuous time series, y_t , can be made discrete by a symbolic recoding method, as described by following expression.

$$S_t = \begin{cases} 1 & \text{for } y_t \leq q_1 \\ 2 & \text{for } q_1 < y_t \leq q_2 \\ \vdots & \\ n-1 & \text{for } q_{n-1} < y_t \leq q_n \\ n & \text{for } y_t \geq q_n \end{cases} \tag{9}$$

At the end of this procedure, each value in the continuous data is assigned to a number between 1 and n .

2.2. Network Analysis

In the field of network analysis, several metrics which describe the properties of networks are proposed by Jackson [19] and Newman [20]. In this context, some metrics describe networks' macrostructure and some metrics describe nodes' micro properties. Examples of these micro metrics are centrality measures. Centrality measures quantify centrality and the importance of nodes by assigning a value to each node. There are many centrality measures proposed in the literature. Some examples are degree centrality, closeness centrality, betweenness centrality, closeness centrality, eigenvector centrality, and PageRank. In this work, we discuss eigenvector centrality and PageRank. Another network analysis method is community detection. In community detection, nodes of the network are partitioned into communities such that, in each community, the nodes are densely connected.

2.2.1. Eigenvector Centrality

The most basic centrality measure is degree centrality. Degree centrality only takes into account the number of edges that a node has. However, the importance of a node's neighbors can be different. Eigenvector centrality takes these differences into account. If a node's neighboring nodes have high centrality (importance), then this node's centrality (importance) should be high too. Eigenvector centrality is proposed by Bonacich [21]. The eigenvector centrality of a node x_i is proportional to the sum of its neighbors' centralities. Eigenvector centrality can be expressed in the formula below:

$$x_i = \kappa^{-1} \sum_{\substack{\text{nodes } j \text{ that are} \\ \text{neighbors of } i}} x_j \quad (10)$$

In the expression above, κ^{-1} is the proportionality constant. The expression above can be rewritten using adjacency matrix A_{ij} of the network, as below:

$$x_i = \kappa^{-1} \sum_{j=1}^n A_{ij} x_j \quad (11)$$

This expression can be stated in matrix notation, as below:

$$\mathbf{Ax} = \kappa \mathbf{x} \quad (12)$$

In the expression above, \mathbf{x} is the eigenvector of the adjacency matrix \mathbf{A} , and its elements are the centrality values.

2.2.2. PageRank

PageRank is a centrality metric which constitutes the core algorithm of Google's search engine [22]. PageRank is associated with eigenvector centrality and designed for directed networks. To determine the centrality of a node, the PageRank algorithm takes three different factors into account. These are the number of nodes that link to the target, the PageRank centrality of the linking nodes, and the link propensity of the linking nodes. PageRank is calculated with the following formula:

$$\mathbf{x} = (\mathbf{I} - \alpha \mathbf{AD}^{-1})^{-1} \mathbf{1} \quad (13)$$

In the expression above, α is a positive constant, $\mathbf{1}$ is the uniform vector $(1, 1, 1, \dots)$, \mathbf{D} is a diagonal matrix with the elements $D_{ii} = \max(k_i^{\text{out}}, 1)$ (k_i^{out} is the outdegree of the node), \mathbf{A} is the adjacency matrix, and \mathbf{I} is the identity matrix.

2.2.3. Community Detection

Blondel et al. [23] proposed an algorithm for community detection in large networks. This algorithm is also known as the Louvain algorithm. This algorithm consists of two phases, namely the modularity optimization and community aggregation phases. These two phases are iteratively repeated until a convergence. In the first phase, modularity optimization, each node is assigned to a different community. Then, each node, i , and its neighbors, j , are considered, and an evaluation is performed to determine whether or not modularity will increase if node i is assigned to the community of j . If so, then node i is assigned to the community of j so that the increase in modularity is maximized. This process is repeated until there is no gain in modularity. The increase in modularity when node i is assigned to a community, C , is denoted with ΔQ and computed with the following formula:

$$\Delta Q = \left[\frac{\sum_{in} + k_{i,in}}{2m} - \left(\frac{\sum_{tot} + k_i}{2m} \right)^2 \right] - \left[\frac{\sum_{in}}{2m} - \left(\frac{\sum_{tot}}{2m} \right)^2 - \left(\frac{k_i}{2m} \right)^2 \right] \quad (14)$$

In the expression above: \sum_{in} denotes the sum of the weight for links in the community C ; \sum_{tot} denotes the sum of the weight for links in relation to nodes in the community C ; k_i denotes the sum of the weight for links connected to node i ; $k_{i,in}$ denotes the sum of the weight for links from node i to nodes in the community C ; and m denotes the sum of the weight for all links in the network.

In the second step, community aggregation, nodes falling in the same community are treated as a single node and a new network is constructed whose nodes comprise the communities from the previous phase. Then, the first step of modularity optimization is executed on the new network. These phases are carried out iteratively until the community structure does not change.

3. Results

In this study, we used effective transfer entropy to create a causality network that comprised COVID-19 data from seventy countries. This network is a weighted directed network where the weights of the links correspond to the strength of causality. The links are measured using effective transfer entropy. After constructing the causality network, we analyzed it using network analysis methods such as eigenvector centrality, PageRank, and the Louvain community detection algorithm.

The data used in this study were obtained from the World Health Organization (WHO). The data contain daily new cases for COVID-19 from seventy different countries and cover dates between 3 January 2020 and 7 January 2022 [24]. WHO data for COVID-19 are organized as a table. In this table, the rows indicate days and the columns indicate variables, such as country code, country, new cases, cumulative cases, new deaths, and cumulative deaths. In this study, we use the new cases data from this data table. We present summary statistics for the daily new cases data from each country in Appendix A. Transfer entropy calculations are performed with the RTransferEntropy package of R software [11]. Network analysis and visualization are performed using the Gephi [25] and igraph packages of R software [26].

The parameters for transfer entropy calculations are determined as follows: Markov orders for time series are set at one; the number of bootstrap replications used in the evaluation of statistical significance for transfer entropies is set at 300; the number of shuffles used in the calculation of effective transfer entropies is set at 100; and the quantiles used in discretization processes are set at 5% and 95%. For transfer entropy to be applicable, the time series must be stationary. We take the first difference from the daily new cases time series to ensure that the time series are stationary. With augmented Dickey–Fuller tests, we verified that the different time series are stationary.

A graph of the constructed causality network is presented in Figure 1. In this network, only statistically significant transfer entropies are plotted. To improve the visibility, Figures 2 and 3 are presented with some arcs filtered according to their weights. In Figure 2, only the arcs whose weights are greater than 0.05 are plotted, and in Figure 3, only the arcs whose weights are greater than 0.06 are plotted. Therefore, in these figures, only the most important causalities are presented. Arrows showing the directional arcs are better seen in these additional figures. High-definition image files of Figures 1–3 and a Pajek network data file of our causality network are provided in the Supplementary Materials section. The obtained causality network is a directed weighted network. Directions in the network indicate the directions of causality, and weights in the network reflect the strength of the causality measured with effective transfer entropy. As seen in Figure 1, there is a giant component and an isolated small component in the network. The small component includes the following countries: Egypt, Iraq, Iran, Kuwait, Lebanon, Libya, Pakistan, Qatar, Saudi Arabia, the Syrian Arab Republic, and Tunisia. Notably, these are Islamic countries. There are causalities between these Islamic countries but there are no causality relationships between these Islamic countries and other countries. This is a novel and interesting finding of our study.

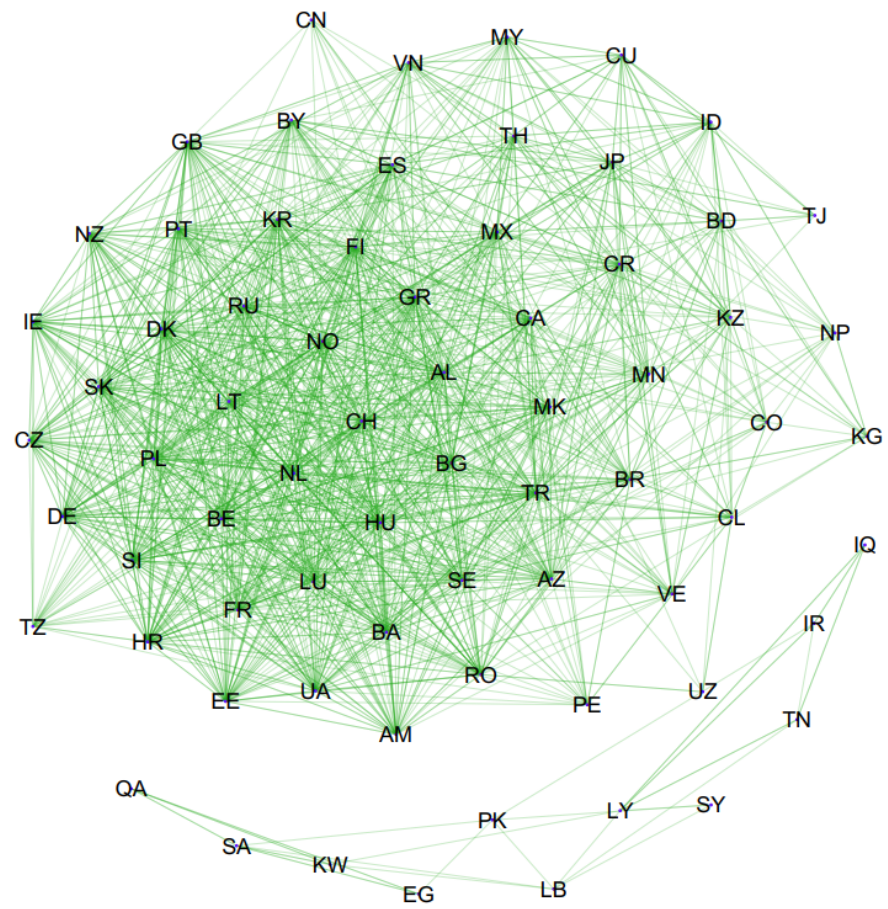


Figure 1. Causality network among seventy countries for COVID-19 using effective transfer entropy.

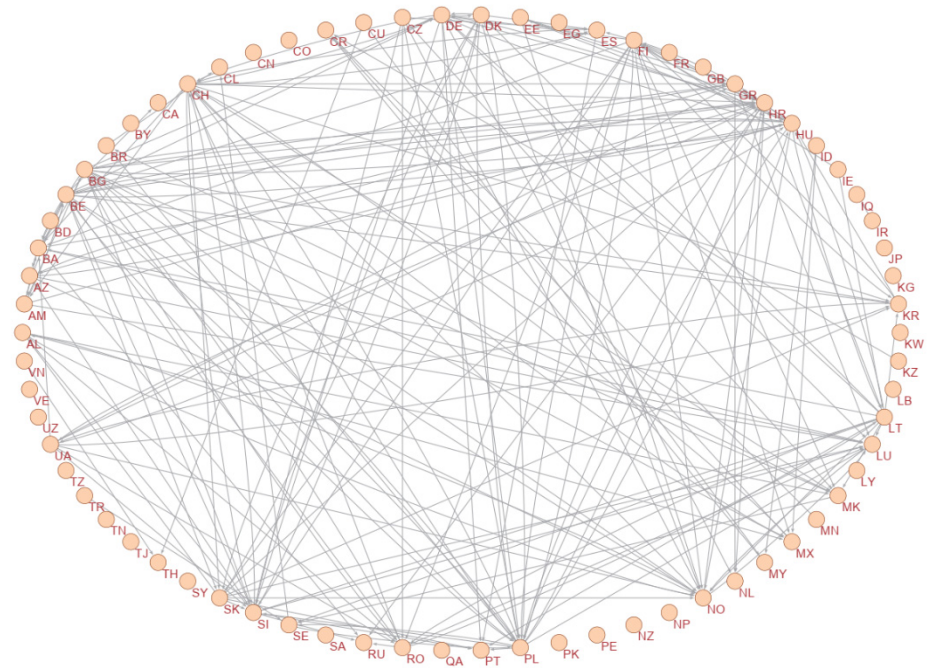


Figure 2. Filtered causality network: Only arcs whose weights are greater than 0.05 are plotted.

Table 1. Cont.

Country	Eigenvector Centrality	PageRank	Country	Eigenvector Centrality	PageRank
Belgium (BE)	0.537333	0.017652	Libya (LY)	0.628994 *	0.011452
Bulgaria (BG)	0.473694	0.016037	North Macedonia (MK)	0.384132	0.014058
Brazil (BR)	0.200907	0.016291	Mongolia (MN)	0.117887	0.010454
Belarus (BY)	0.296759	0.014259	Mexico (MX)	0.273776	0.015344
Canada (CA)	0.288521	0.013702	Malaysia (MY)	0.048075	0.010252
Switzerland (CH)	0.592722	0.021829	Netherlands (NL)	0.465379	0.017194
Chile (CL)	0.125363	0.016200	Norway (NO)	1.000000	0.033528
China (CN)	0.010420	0.003341	Nepal (NP)	0.020155	0.005171
Colombia (CO)	0.040071	0.005974	New Zealand (NZ)	0.253361	0.010018
Costa Rica (CR)	0.194700	0.020956	Peru (PE)	0.079954	0.006499
Cuba (CU)	0.029443	0.009441	Pakistan (PK)	0.123575 *	0.007852
Czechia (CZ)	0.374990	0.013695	Poland (PL)	0.797845	0.024624
Germany (DE)	0.584266	0.019286	Portugal (PT)	0.495055	0.018178
Denmark (DK)	0.472643	0.015801	Qatar (QA)	0.088225 *	0.012552
Estonia (EE)	0.434803	0.014688	Romania (RO)	0.609940	0.020255
Egypt (EG)	0.071470 *	0.009371	Russian Federation (RU)	0.598568	0.021318
Spain (ES)	0.364177	0.017179	Saudi Arabia (SA)	0.117345 *	0.013353
Finland (FI)	0.578325	0.021833	Sweden (SE)	0.518638	0.020728
France (FR)	0.287441	0.013241	Slovenia (SI)	0.960990	0.029255
United Kingdom (GB)	0.252125	0.011740	Slovakia (SK)	0.524288	0.018905
Greece (GR)	0.634762	0.023944	Syrian Arab Republic (SY)	0.144949 *	0.010396
Croatia (HR)	0.949647	0.029384	Thailand (TH)	0.093885	0.012641
Hungary (HU)	0.738304	0.023563	Tajikistan (TJ)	0.010324	0.004028
Indonesia (ID)	0.029716	0.008124	Tunisia (TN)	0.565851	0.008409
Ireland (IE)	0.232775	0.009269	Turkey (TR)	0.307547	0.014783
Iraq (IQ)	1.000000 *	0.012495	Tanzania (TZ)	0.059911	0.004068
Iran (IR)	0.552977 *	0.009154	Ukraine (UA)	0.364791	0.013043
Japan (JP)	0.076052	0.009334	Uzbekistan (UZ)	0.007412	0.003278
Kyrgyzstan (KG)	0.003818	0.004563	Venezuela (VE)	0.060501	0.005083
Korea (KR)	0.543237	0.023837	Vietnam (VN)	0.340229	0.009294

* Eigenvector centrality values for Egypt, Iraq, Iran, Kuwait, Lebanon, Libya, Pakistan, Qatar, Saudi Arabia, Syrian Arab Republic, and Tunisia are calculated from subnetwork.

Table 2. Community affiliation of node countries.

Community 1	Community 2	Community 3	Community 4
Armenia (AM)	Albania (AL)	Egypt (EG)	Bangladesh (BD)
Azerbaijan (AZ)	Belarus (BY)	Iraq (IQ)	Brazil (BR)
Bosnia and Herzegovina (BA)	China (CN)	Iran (IR)	Chile (CL)
Belgium (BE)	Czechia (CZ)	Kuwait (KW)	Colombia (CO)
Bulgaria (BG)	Germany (DE)	Lebanon (LB)	Costa Rica (CR)
Canada (CA)	Denmark (DK)	Libya (LY)	Cuba (CU)
Switzerland (CH)	Estonia (EE)	Pakistan (PK)	Indonesia (ID)
Luxembourg (LU)	Spain (ES)	Qatar (QA)	Japan (JP)
North Macedonia (MK)	Finland (FI)	Saudi Arabia (SA)	Kyrgyzstan (KG)
Netherlands (NL)	France (FR)	Syrian Arab Republic (SY)	Kazakhstan (KZ)
Norway (NO)	United Kingdom (GB)	Tunisia (TN)	Mongolia (MN)
Poland (PL)	Greece (GR)		Mexico (MX)
Romania (RO)	Croatia (HR)		Malaysia (MY)
Sweden (SE)	Hungary (HU)		Nepal (NP)
Turkey (TR)	Ireland (IE)		Peru (PE)
Ukraine (UA)	Korea (KR)		Thailand (TH)
Venezuela (VE)	Lithuania (LT)		Tajikistan (TJ)
	New Zealand (NZ)		Uzbekistan (UZ)
	Portugal (PT)		Vietnam (VN)
	Russian Federation (RU)		
	Slovenia (SI)		
	Slovakia (SK)		
	Tanzania (TZ)		

4. Conclusions

In this study, we constructed a causality network for COVID-19 including seventy countries. In this construction, an information-theory-based causality measure, transfer entropy, is utilized. Transfer entropy has some advantages over other causality tests such that it is able to measure the strength of the causality and can detect nonlinear causality relationships. After drawing the causality network, we analyzed it by using centrality measures such as eigenvector centrality and PageRank. We computed the eigenvector centrality and PageRank for each country and presented them in a table. Additionally, we analyzed the community structure in the causality network and detected four distinct communities in the network.

One finding of our study is that there are two clusters: Islamic countries and other countries. In the causality network, we constructed 1637 directed arcs, and for each arc there is a weight value which reveals the strength of the causality. However, it is impossible for us to present these 1637 weight values in our main text. Therefore, we supplied a Pajek network file in the Supplementary Materials section. The Pajek network file we supplied contains 1637 weight values, each corresponding to an arc of the network. Epidemiologists can learn several lessons from our results. For example, in the causality network, if there is a strong causality between one country and another, this means that the first country

strongly spread coronavirus to the second country. In this case, the second country could take additional measures against the first, highly contagious country. Epidemiologists can also use data in our causality network to simulate the spread of coronavirus across countries. In our study, we also presented the centrality of countries in the causality network. Countries with high centrality values are hubs for the spread of coronavirus. Therefore, additional measures can be taken in these hub countries to prevent spread of the coronavirus worldwide. Moreover, we detected four communities in our network. These communities reveal strongly connected countries in terms of the spread of coronavirus, and the transmission rates of the coronavirus between these countries is intense. Finally, our results portray the spreading structure of the coronavirus among countries and will be very useful for epidemiologists.

Supplementary Materials: The following supporting information can be downloaded at: <https://www.mdpi.com/article/10.3390/e24081115/s1>, We provided following files in our supplementary materials compressed zip file. The Pajek network file of Figure 1 is supplied as “Pajek Network File of the Causality Network.net” file. A high-definition PDF file of Figure 1 is supplied as “Figure 1. Causality network.pdf”. High-definition EPS files of Figures 2 and 3 are supplied as “Figure 2. Filtered causality network.eps” and “Figure 3. Filtered causality network.eps”.

Funding: This research received no external funding.

Institutional Review Board Statement: Not applicable.

Informed Consent Statement: Not applicable.

Data Availability Statement: Data were obtained from the WHO website: <https://covid19.who.int/data> (accessed on 7 January 2022).

Conflicts of Interest: The author declares no conflict of interest.

Abbreviations

COVID-19 coronavirus disease 2019

Appendix A

Table A1. Summary statistics for daily new cases data for each country.

Country	1.Q	Median	Mean	3.Q	Max	Country	1.Q	Median	Mean	3.Q	Max
AL	18	149	292	520	1648	KW	52	527	576	886	2246
AM	103	273	469	629	2603	KZ	310	926	1462	1766	10,897
AZ	101	352	842	1215	5048	LB	34	627	1008	1519	6154
BA	38	260	404	644	2154	LT	17	372	729	1216	3926
BD	350	1372	2160	2657	16,230	LU	14	79	150	184	2131
BE	441	1512	2999	3017	27,867	LY	0	440	533	748	4322
BG	65	332	1046	1709	6816	MK	29	162	313	465	1725
BR	9213	25,322	30,368	46,896	150,106	MN	0	19	533	878	3963
BY	229	944	958	1650	2170	MX	1958	3917	5475	7161	25,346
CA	518	2156	3254	4233	52,548	MY	39	1357	3773	5153	24,599
CH	154	927	1968	2264	31,336	NL	498	2714	4413	6620	24,700
CL	864	1770	2469	3733	36,179	NO	54	262	572	596	8385
CN	26	50	181	107	15,152	NP	108	422	1129	1481	9317
CO	1511	5016	7092	10,142	33,594	NZ	0	3	19	11	222

Table A1. Cont.

Country	1.Q	Median	Mean	3.Q	Max	Country	1.Q	Median	Mean	3.Q	Max
CR	85	588	786	1207	3173	PE	985	2391	3150	4850	13,326
CU	22	98	1319	1057	9907	PK	505	1308	1767	2754	6884
CZ	121	510	3420	5438	27,937	PL	257	758	5695	9068	35,251
DE	812	4652	10,079	14,030	76,414	PT	306	690	2091	2512	39,570
DK	111	494	1249	991	28,283	QA	136	211	347	440	2355
EE	10	126	339	526	2300	RO	217	1144	2484	3528	18,863
EG	136	511	529	870	1774	RU	6333	10,758	14,427	22,784	41,335
ES	1774	5376	9406	10,996	136,047	SA	96	390	769	1146	4919
FI	45	206	415	474	9921	SE	276	784	1869	2721	17,320
FR	1118	5878	14,813	19,806	329,558	SI	18	247	651	1042	4518
GB	1734	6591	19,042	30,923	218,705	SK	18	164	1165	1746	15,278
GR	54	866	1932	2434	50,182	SY	6	50	69	92	442
HR	52	278	1013	1380	9058	TH	5	83	3061	3624	23,418
HU	11	208	1743	2046	27,830	TJ	0	0	24	41	407
ID	435	3184	5795	6217	56,757	TN	12	397	995	1454	9823
IE	125	437	1235	1285	23,817	TR	2766	8402	13,297	21,706	68,413
IQ	554	2229	2851	4315	13,515	TZ	0	0	42	0	24,307
IR	2245	6151	8437	11,414	50,228	UA	574	2564	5022	7961	27,377
JP	179	851	2369	2579	26,050	UZ	57	212	271	408	974
KG	44	104	252	334	1965	VE	184	523	606	1009	1939
KR	63	438	893	1108	7850	VN	1	8	2505	1046	39,132

References

- Granger, C.W. Investigating causal relations by econometric models and cross-spectral methods. *Econom. J. Econom. Soc.* **1969**, *37*, 424–438. [\[CrossRef\]](#)
- Toda, H.Y.; Yamamoto, T. Statistical inference in vector autoregressions with possibly integrated processes. *J. Econom.* **1995**, *66*, 225–250. [\[CrossRef\]](#)
- Hatemi, J.A. Asymmetric causality tests with an application. *Empir. Econ.* **2012**, *43*, 447–456. [\[CrossRef\]](#)
- Hiemstra, C.; Jones, J.D. Testing for linear and nonlinear Granger causality in the stock price-volume relation. *J. Financ.* **1994**, *49*, 1639–1664.
- Breitung, J.; Candelon, B. Testing for short-and long-run causality: A frequency-domain approach. *J. Econom.* **2006**, *132*, 363–378. [\[CrossRef\]](#)
- Diks, C.; Panchenko, V. A new statistic and practical guidelines for nonparametric Granger causality testing. *J. Econ. Dyn. Control.* **2006**, *30*, 1647–1669. [\[CrossRef\]](#)
- Lento, C.; Gradojevic, N. S&P 500 index price spillovers around the COVID-19 market meltdown. *J. Risk Financ. Manag.* **2021**, *14*, 330.
- Schreiber, T. Measuring information transfer. *Phys. Rev. Lett.* **2000**, *85*, 461. [\[CrossRef\]](#) [\[PubMed\]](#)
- Paluš, M.; Komárek, V.; Hrnčíř, Z.; Štěrbová, K. Synchronization as adjustment of information rates: Detection from bivariate time series. *Phys. Rev. E* **2001**, *63*, 046211. [\[CrossRef\]](#) [\[PubMed\]](#)
- He, J.; Shang, P. Comparison of transfer entropy methods for financial time series. *Phys. A Stat. Mech. Its Appl.* **2017**, *482*, 772–785. [\[CrossRef\]](#)
- Behrendt, S.; Dimpfl, T.; Peter, F.J.; Zimmermann, D.J. RTransferEntropy—Quantifying information flow between different time series using effective transfer entropy. *SoftwareX* **2019**, *10*, 100265. [\[CrossRef\]](#)
- Adam, A.M. Susceptibility of stock market returns to international economic policy: Evidence from effective transfer entropy of Africa with the implication for open innovation. *J. Open Innov. Technol. Mark. Complex.* **2020**, *6*, 71. [\[CrossRef\]](#)
- Jizba, P.; Lavička, H.; Tabachová, Z. Rényi Transfer Entropy Estimators for Financial Time Series. *Eng. Proc.* **2021**, *5*, 33.
- Assaf, A.; Bilgin, M.H.; Demir, E. Using transfer entropy to measure information flows between cryptocurrencies. *Phys. A Stat. Mech. Its Appl.* **2022**, *586*, 126484. [\[CrossRef\]](#)

15. Shannon, C.E.; Weaver, W. *The Mathematical Theory of Information*; University of Illinois Press: Urbana, IL, USA, 1949.
16. Kullback, S. *Information Theory and Statistics*; Wiley: New York, NY, USA, 1959.
17. Marschinski, R.; Kantz, H. Analysing the information flow between financial time series. *Eur. Phys. J. B-Condens. Matter Complex Syst.* **2002**, *30*, 275–281. [[CrossRef](#)]
18. Dimpfl, T.; Peter, F.J. Using transfer entropy to measure information flows between financial markets. *Stud. Nonlinear Dyn. Econom.* **2013**, *17*, 85–102. [[CrossRef](#)]
19. Jackson, M.O. *Social and Economic Networks*; Princeton University: Princeton, NJ, USA, 2008.
20. Newman, M. *Networks*; Oxford University Press: Oxford, UK, 2018.
21. Bonacich, P. Some unique properties of eigenvector centrality. *Soc. Netw.* **2007**, *29*, 555–564. [[CrossRef](#)]
22. Page, L.; Brin, S.; Motwani, R.; Winograd, T. *The PageRank Citation Ranking: Bringing Order to the Web*; Stanford InfoLab: Stanford, CA, USA, 1999.
23. Blondel, V.D.; Guillaume, J.L.; Lambiotte, R.; Lefebvre, E. Fast unfolding of communities in large networks. *J. Stat. Mech. Theory Exp.* **2008**, *2008*, P10008. [[CrossRef](#)]
24. World Health Organization. WHO Coronavirus (COVID-19) Dashboard. 2021. Available online: <https://covid19.who.int/info> (accessed on 7 January 2022).
25. Bastian, M.; Heymann, S.; Jacomy, M. Gephi: An open source software for exploring and manipulating networks. *Int. AAAI Conf. Weblogs Soc. Media* **2009**, *3*, 361–362.
26. Csardi, G.; Nepusz, T. The Igraph Software Package for Complex Network Research. *Interj. Complex Syst.* **2006**, *1695*, 1–9. Available online: <https://igraph.org> (accessed on 20 July 2022).